Evidence of dynamic Jahn-Teller effects in ferromagnetism of rhombohedral Al-substituted lanthanum manganite

2000 J. Phys.: Condens. Matter 12 3835

(http://iopscience.iop.org/0953-8984/12/16/306)

J. Phys.: Condens. Matter **12** (2000) 3835–3847. Printed in the UK PII: S0953-8984(00)11395-5

Evidence of dynamic Jahn–Teller effects in ferromagnetism of rhombohedral Al-substituted lanthanum manganite

R V Krishnan and A Banerjee

Inter University Consortium for DAE Facilities, University Campus, Khandwa Road, Indore 452 017, India

Received 27 January 2000

Abstract. We report the structural, magnetic and electron transport properties of a new series of compounds where we have substituted Al^{3+} in the Mn site of rhombohedral, cation deficient $LaMnO_{3+\delta}$. All the samples crystallize in rhombohedral ($R\bar{3}c$) symmetry with minimal changes in lattice parameters. Mn^{4+} content gradually decreases from ∼25% with increase in Al content and samples with $x \geqslant 15\%$ are stoichiometric without any detectable Mn^{4+}. A gradual transition from the ferromagnetic–metallic state to ferromagnetic–insulating state is observed with increase in Al substitution. This indicates a progressive crossover from the double exchange dominated regime indicated by metallicity to the superexchange regime indicated by the absence of Mn^{4+} across the series. Ferromagnetism in the samples with no Mn^{4+} is because of ferromagnetic Mn^{3+}–O–Mn^{3+} interactions which is possible in the presence of dynamic Jahn–Teller effects in $R\bar{3}c$ symmetry. A semiquantitative estimate of T_C was carried out on the basis of near-neighbour exchange interactions and a good agreement with the observed T_C is reported. Through this the importance of dynamic Jahn–Teller effects coupled with Mn^{3+}–O–Mn^{3+} interactions giving rise to ferromagnetism is shown for the whole series. Samples with $x \geqslant 7.5\%$ show a second transition in ac susceptibility at lower temperatures and from the preliminary measurements their origin is attributed to the dynamics of small ferromagnetic clusters arising due to random Al substitution in some of the infinite ferromagnetic matrix.

1. Introduction

The structural, magnetic and transport properties of hole doped $LaMnO_{3+\delta}$ and $La_{1-x}D_xMnO_3$ ($D = Ca^{2+}$, Sr^{2+}, Ba^{2+}) depend on the MnO_6 octahedron and its variations upon doping. The long range chemical bonding of these MnO_6 octahedral networks, the Mn–O–Mn bond angles, Mn–O bond distances and more important, the Mn^{3+}/Mn^{4+} ratio, all of these influence cooperatively the structural, magnetic and transport properties in these materials which show interesting and important physical phenomena such as colossal magnetoresistance (CMR), charge and orbital ordering, spontaneous phase segregation etc [1–6]. An important aspect of these manganites is that the properties depend crucially on the nature and magnitude of the distortions from the perfect cubic symmetry. For instance, the orthorhombic samples are always found to be insulating while rhombohedral and cubic samples exhibit a metal–insulator transition (MIT) although ferromagnetism is observed in all the three structures. The structure and in turn, the magnetic and electronic properties of these manganites are influenced by two major factors namely, the Goldschmidt tolerance factor 't' and the Jahn–Teller (JT) distortion [5, 6].

The distortion of the structure from cubic symmetry is accompanied by the deviation of 't' from unity indicating compressional or tensile stresses in various bonds. These structural

0953-8984/00/163835+13$30.00

stresses resulting from $t < 1$ in $LnMnO_3$ can be partially removed by cooperative rotation of MnO_6 octahedra around different cubic axes giving rise to rhombohedral and orthorhombic structures. Such a rotation changes the Mn–O–Mn bond angle from 180° which profoundly affects the magnetic interactions and electron transfer. The structural stresses in orthorhombic stoichiometric $LnMnO_3$ can be lessened by oxidation of MnO_6 array because of the reduction of Mn–O equilibrium bond lengths resulting from the removal of e_g electron from Mn^{3+} [6]. Following the same logic, the structural stresses can also be released by the replacement of Mn^{3+} (0.645 Å) by a smaller ion like Al^{3+} (0.535 Å) resulting in more symmetric rhombohedral structure. The JT instability arises out of the twofold orbital degeneracy of Mn^{3+} leading to optical breathing-mode vibration of oxygen atoms on either side of the Mn^{3+} ion. Elastic coupling of these vibrations at individual sites stabilizes cooperative local distortions which can be static or dynamic, long range or short range. Stoichiometric $LaMnO_3$ stabilizes in orthorhombic structure with long range static JT distortions below a orthorhombic–rhombohedral transition temperature giving rise to an antiferromagnetic insulating phase [3, 4]. The oxidation of the MnO_6 array (i.e hole doping) reduces the JT ion Mn^{3+} by introducing the Mn^{4+} leading to progressively more symmetric rhombohedral and cubic structures that remain stable even to the lowest temperatures. The hole doped $LaMnO_3$, commonly written as $LaMnO_{3+\delta}$ but actually cation deficient $La_{1-\lambda}Mn_{1-\lambda}O_3$, stabilizes in $R\bar{3}c$ symmetry with a reasonable decrease in Mn^{3+} ions, exhibiting a MIT accompanied by a ferromagnetic transition [5]. This has all the ingredients of a prototype CMR manganite and thus can be considered as a parent compound for them. The $R\bar{3}c$ symmetry does not support static JT distortion because of the competition between electrostatic and elastic energies but the breathing mode displacement of oxygen continues to persist giving rise to what is known as dynamic Jahn–Teller distortion [6–8]. Although ferromagnetism and metallicity in hole doped manganites are explained qualitatively on the basis of Zener's double exchange (DE) mechanism [9], there are quantitative discrepancies in the observed T_C and resistivity behaviour, from the predictions of the above model. Recent theoretical and experimental studies indicate that Zener DE is not adequate [10–13]. The observed dynamic JT effect or electron–lattice interaction is currently understood to be an important ingredient for any theory to explain the physical properties of CMR manganites. The importance of the dynamic JT effect has already been highlighted in the earlier work of Goodenough *et al* and there it was shown to be the responsible mechanism for ferromagnetic Mn^{3+}–O–Mn^{3+} interactions in $LaMn_{1-x}Ga_xO_3$ [7]. Some of the recent works in systems where there is no heterovalence of the Mn and hence no DE, have shown large CMR questioning the necessity of the DE framework for the explanation of ferromagnetism and CMR in manganites [14]. In essence these studies have signified the pertinence of ferromagnetic superexchange (SE) interactions coupled with the dynamic JT effect in manganites. Hence there is a need to explicate the relative importance of DE and SE interactions in the presence of the dynamic JT effects for the explanation of ferromagnetism and metallicity in prototype CMR manganites. It is found that the dynamic JT effect is dominant in more symmetric structures which cannot afford a long range, cooperative static JT distortion [7, 8]. Here enters the importance of rhombohedral structure which supports the dynamic JT distortions and not the static JT distortions unlike the orthorhombic structure which supports both [2, 6, 11]. In this regard it will be more relevant and meaningful to study a series of rhombohedral compounds where the ferromagnetic DE interactions and metallic bonds are systematically diluted by decreasing the Mn^{4+} content with a nonmagnetic dopant but simultaneously maintaining the same crystal symmetry devoid of any other lattice complications (ionic size mismatch etc) so that one can study the transition across both the observed ferromagnetic (6–12% Mn^{4+}) and conduction (∼12–16% Mn^{4+}) percolation thresholds [5].

With this motivation we have chosen to substitute Al^{3+} in the Mn site of the rhombohedral, cation deficient $LaMnO_{3+\delta}$. It is worthy of note that this particular substitution has never been studied in rhombohedral structure. The parent compound has DE dominated ferromagnetism and MIT arising from Mn^{3+}–O–Mn^{4+} interactions [5]. Since both the end members of the series, i.e., $LaMnO_{3+\delta}$ and $LaAlO_3$, crystallize in the $R\bar{3}c$ symmetry, Al substitution is expected to maintain the rhombohedral symmetry throughout the doping range, introducing no structural changes or other lattice complications as observed in some of the earlier works [15, 16]. Because of the similar ionic sizes of Al^{3+} (0.535 Å) and Mn^{4+} (0.530 Å), Al substitution is also expected to gradually reduce the Mn^{4+} content, thereby reducing the strength of DE. Thus a systematic dilution of ferromagnetism is expected by virtue of the variation of relative strengths of DE and SE interactions in the same $R\bar{3}c$ symmetry.

We present below the results of low field magnetic and resistivity measurements on the series $LaMn_{1-x}Al_xO_{3+\delta}$ with $0.0 \leqslant x \leqslant 0.2$. The whole series of compounds crystallize in $R\bar{3}c$ symmetry with only slight variations in lattice parameters and rhombohedral distortion. All the samples are found to exhibit a ferromagnetic transition with Curie temperatures decreasing progressively with Al doping. Lower doped samples ($x \leqslant 5\%$) exhibit MIT near T_C whereas the sample with $x = 7.5\%$ shows a tendency for MIT but becomes semiconducting at lower temperatures. The samples with $x \geqslant 10\%$ are all semiconducting. Thus we observe a gradual crossover from ferromagnetic metal (FMM) phase to ferromagnetic insulating (FMI) phase suggesting a crossover from DE to SE regime within the same crystal symmetry. Such a composition-driven transition from FMM to FMI state within the same structure probably cannot be found in the literature on lanthanum manganites.

A semiquantitative estimate of the ferromagnetic T_C using near-neighbour interaction strengths is obtained for all the samples and a reasonably good agreement with experimental values is reported. In this analysis the importance of ferromagnetic Mn^{3+}–O–Mn^{3+} interactions assisted by dynamic JT effects is highlighted. We also observe a progressive setting in of a second magnetic phase at low temperatures for $x \geqslant 7.5\%$ samples. Though at present we concentrate mainly on the ferromagnetic transition we discuss briefly the plausible origin of this second transition too. To the best of our knowledge, this series forms an unique platform to study the continuous transition from ferromagnetic metal to ferromagnetic insulator state and the progressive decrease of DE interactions in the presence of dynamic JT effects in the same crystal symmetry.

2. Experiment

Polycrystalline samples of the series $LaMn_{1-x}Al_xO_{3+\delta}$ with $0 \leqslant x \leqslant 20\%$ have been prepared by the standard solid state ceramic route with ($\geqslant$99.9% pure) starting materials La_2O_3, MnO_2 and Al_2O_3. The powdered samples were sintered at around 950 °C for 24 hours. The sintered samples were cooled slowly to room temperature and were reground and pelletized and a similar heat treatment was given thrice. The final sintering was given at around 1250 °C in air for 48 hours and samples were cooled slowly to 1040 °C and then were kept in oxygen flow for about 24 hours. Some of the compositions of low Al content were also prepared by the nitrate route where a more homogeneous mixing of the reactants is expected. These samples have the same structural parameters with almost the same peak values of resistivity and susceptibility having the same transition temperatures as those of the samples prepared by ceramic route. X-ray diffraction (XRD) measurements were made using a Rigaku Rotaflex RTC 300 RC powder diffractometer with Cu Kα radiation. The patterns were collected in the range of 10–90° at the interval of 0.01°. The XRD patterns were analysed by the Rietveld profile refinement method using the modified version of the profile refinement program by Young *et al* [17]. Iodometric

redox titrations using sodium thiosulphate and potassium iodide were done to estimate the oxygen non-stoichiometry. Usually the excess oxygen is incorporated in the realistic chemical formula as metal ion vacancies. Thus the chemical formula of our samples $LaMn_{1-x}Al_xO_{3+\delta}$ is proposed as $La_{1-\lambda}(Mn_{1-x}Al_x)_{1-\lambda}O_3$ where λ is the amount of cation vacancies which is related to the oxygen non-stoichiometry by the relation $\lambda = (\delta/(3+\delta))$. In our Rietveld profile refinement we have consistently taken into account this factor while refining the composition in all the samples. This matches well with that obtained from iodometry. We have assumed equal amounts of vacancies in La and Mn sites in line with the earlier studies [18]. Low field dc magnetization as well as linear and nonlinear ac susceptibility measurements were done using home-made setups [19, 20]. Dc resistance and low frequency (∼33.33 Hz) ac resistance measurements were done in the standard four-probe geometry.

3. Results and discussion

Figure 1 shows the representative XRD patterns of the compositions $x = 0$, 5, 10 and 15% in the series $(LaMn_{1-x}Al_x)_{1-\lambda}O_3$. All the samples crystallize in the rhombohedral ($R\bar{3}c$) symmetry with only a slight distortion i.e. $\alpha = 60^\circ + \Delta\alpha$. This distortion and the unit cell volume slightly decrease with Al substitution but cause no appreciable lattice effects due to substitution. Iodometry and an independent Rietveld profile refinement of the XRD patterns of the samples reveal that there is a decrease in Mn^{4+} content with Al substitution. Hence we observe that the samples with higher Al content ($x \geqslant 15\%$) have no Mn^{4+} in the lattice and are stoichiometric satisfying the Goldschmidt tolerance factor. Figure 2(a) gives the temperature dependence of the real part (χ') of ac susceptibility for all the samples measured in 80 mOe field and at 133.33 Hz. All the samples undergo a transition from paramagnetic to ferromagnetic phase at a well defined T_C marked by a concomitant increase in the magnetic susceptibility. The T_C values were determined from the inflexion points of the $\chi'(T)$ curves. Hence we observe a systematic decrease in the transition temperature T_C with increasing Al substitution. Figure 2(b) gives the imaginary part (χ'') of ac susceptibility for a few samples of the series showing the peaks associated with ferromagnetic losses at the respective transitions. Figure 3 shows the second order ac susceptibility which is a testimony to a symmetry breaking field resulting from the spontaneous magnetization in the ferromagnetic phase. Figure 4 shows the fitting of experimental data to the Curie–Weiss law in the paramagnetic region. The paramagnetic moments calculated from the Curie–Weiss law fits (μ_{eff}) for all the samples remain lower than the calculated spin-only values ($=g[S(S+1)]^{1/2}\mu_B$) as seen in the inset of figure 4. A similar observation has been made by Goodenough *et al* in both $LaMnO_{3+\delta}$ and in $LaMn_{1-x}Ga_xO_3$ [7]. This had been attributed to the substantial anisotropic SE interaction between Mn^{3+}–Mn^{3+} pairs as well as to the disorder in the Mn sublattice. The positive values of θ from Curie–Weiss law fits in all the samples suggest mean-field ferromagnetic interactions. Figure 5 gives the representative Arrott plots based on the method given in [21] for the sample with $x = 20\%$. The posive intercepts on the y axis of Arrott plots point to the existence of spontaneous magnetization in the sample below $T_C \sim 126$ K. This, together with the observation of opposite curvatures above and below T_C strongly suggest ferromagnetism in the $x = 20\%$ sample which does not have any DE ferromagnetic interactions. Table 1 summarizes the structural and magnetic parameters obtained for all the compositions in our series. Figures 6(a) and (b) show the temperature dependence of resistivity of the samples. The dc and low frequency resistivities overlap over the whole temperature range, indicating that the measured resistivity is intrinsic to the samples. While the samples with $x \leqslant 5\%$ show the metal–insulator transition around the ferromagnetic T_C, the sample with $x = 7.5\%$ shows a tendency to MIT around T_C but subsequently becomes semiconducting at low temperature.

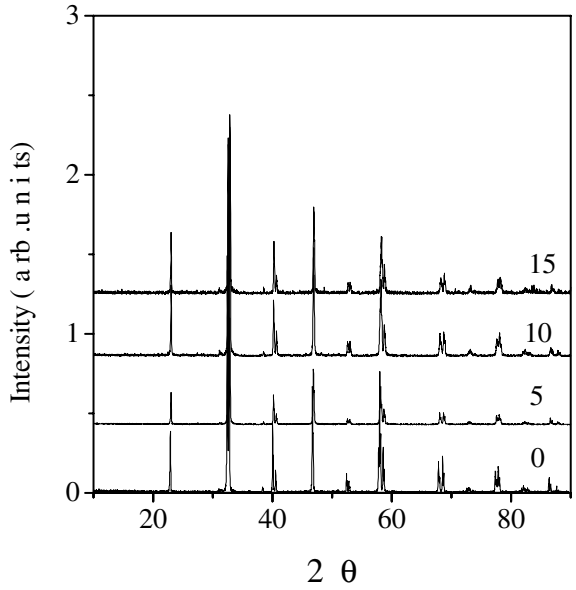

Figure 1. Representative XRD patterns of $x = 0$, 5, 10 and 15% samples of series $LaMn_{1-x}Al_xO_{3+\delta}$. All the samples in the series crystallize in rhombohedral ($R\bar{3}c$) symmetry.

Table 1. Structural and magnetic parameters for the series $LaMn_{1-x}Al_xO_{3+\delta}$

	$x = 0.0$	$x = 0.025$	$x = 0.05$	$x = 0.075$	$x = 0.10$	$x = 0.15$	$x = 0.20$
Mn^{3+} (%)	79	73.5	70	78.5	82.6	85	80
Mn^{4+} (%)	21	24	25	14	7.4	0	0
a (Å)	5.4716	5.4691	5.4667	5.4666	5.4641	5.4565	5.4524
V_c (Å^3)	117.33	117.21	116.95	116.97	116.82	116.21	115.87
α (°)	60.57	60.58	60.55	60.56	60.56	60.51	60.48
T_C (K)	234.2	220.5	208.8	187.6	162.0	143.0	126.0
μ_{eff} (μ_B)	3.66	3.58	3.45	3.48	3.56	3.23	2.99
θ (K)	232.5	223.1	218.7	206.2	188.6	178.5	172.3

The samples with $x \geqslant 10\%$ are all semiconducting in the measured temperature range with increasing temperature coefficient of resistivity. Hence with the increase in Al content, there is a progressive transition from ferromagnetic metal to ferromagnetic insulating state within the same structure. For $x \geqslant 7.5\%$ samples, there occurs a second magnetic transition at lower temperatures as can be seen from figures 2(a) and 2(b).

To explain the observed variation of T_C with the Al substitution we attempt to analyse our results in the framework of DE and SE interactions with dynamic Jahn–Teller (JT) effects. The magnetic phases that result in the case of manganites are effectively a balance between these DE and SE interactions. This balance crucially depends on the Mn^{3+}/Mn^{4+} ratio resulting from hole doping as well as on the local structural variations of the MnO_6 octahedra due to doping either in the La site or in the Mn site [5]. DE relies on the random distribution of Mn^{4+} and Mn^{3+} ions in the lattice. Thus changes in the content of JT ion Mn^{3+} would influence the ferromagnetic SE interactions and changes in the Mn^{3+}/Mn^{4+} ratio would likewise influence the ferromagnetic DE interactions. In the present case of Al substituted lanthanum manganite, there are three relevant magnetic bonds in the system namely, the Mn^{3+}–O–Mn^{3+},

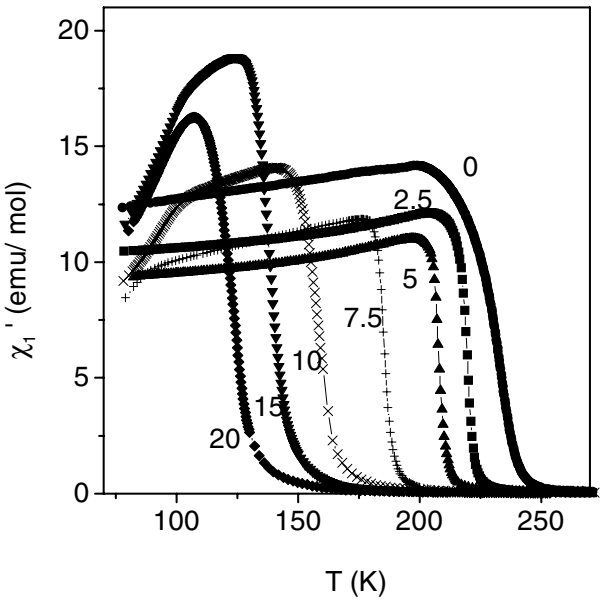

(a)

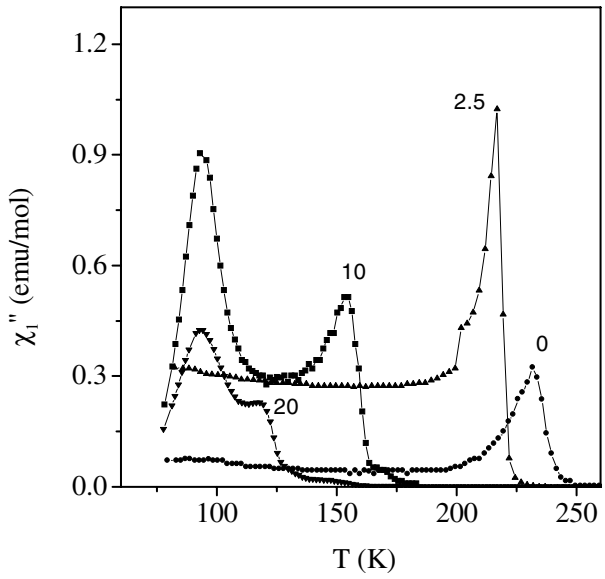

(b)

Figure 2. (a) Temperature dependence of real part (χ') of ac susceptibility of the series $LaMn_{1-x}Al_xO_{3+\delta}$ in 80 mOe field and at 133.33 Hz. (b) Temperature dependence of imaginary part (χ'') of ac susceptibility of the samples with $x = 0$, 2.5, 10, 20% in the series $LaMn_{1-x}Al_xO_{3+\delta}$.

Mn^{4+}–O–Mn^{4+} which are superexchange bonds and Mn^{3+}–O–Mn^{4+} which is the double exchange bond. We define the strength of these three bonds by the exchange constants J_1, J_2 and J_3 respectively as was done by Jonker [1]. Jonker assumed a positive sign for both J_1 and J_3 and a negative sign for J_2. We also follow the same convention for the signs of exchange

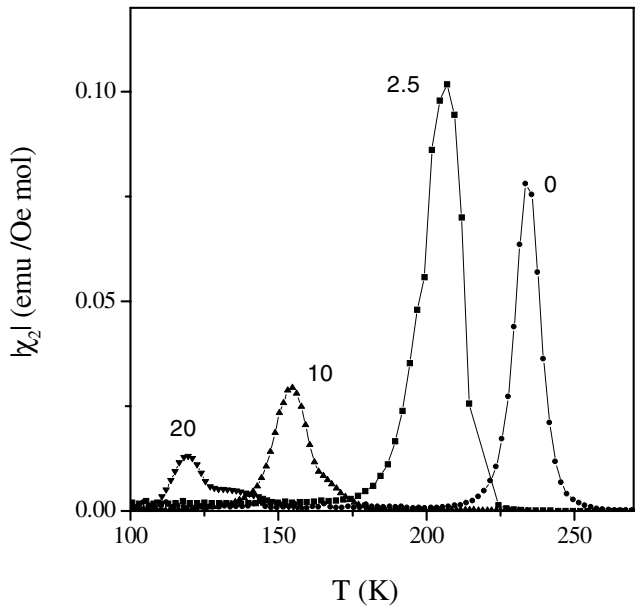

Figure 3. Temperature dependence of second order (χ_2) ac susceptibility of the samples with $x = 0, 2.5, 10, 20\%$ in the series $LaMn_{1-x}Al_xO_{3+\delta}$.

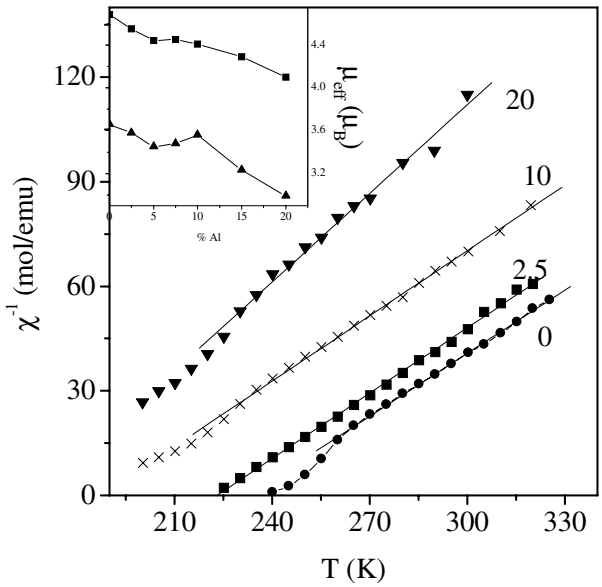

Figure 4. The Curie–Weiss law fits for $x = 0$, 2.5, 10 and 20% samples of the series $LaMn_{1-x}Al_xO_{3+\delta}$. The inset shows the observed (▲) and calculated spin-only (■) values of paramagnetic effective moment.

constants. This is in consensus with the proposal for FM SE interactions in Mn^{3+}–Mn^{3+} made by Goodenough *et al* on the basis of dynamic JT effects [7]. This becomes necessary for

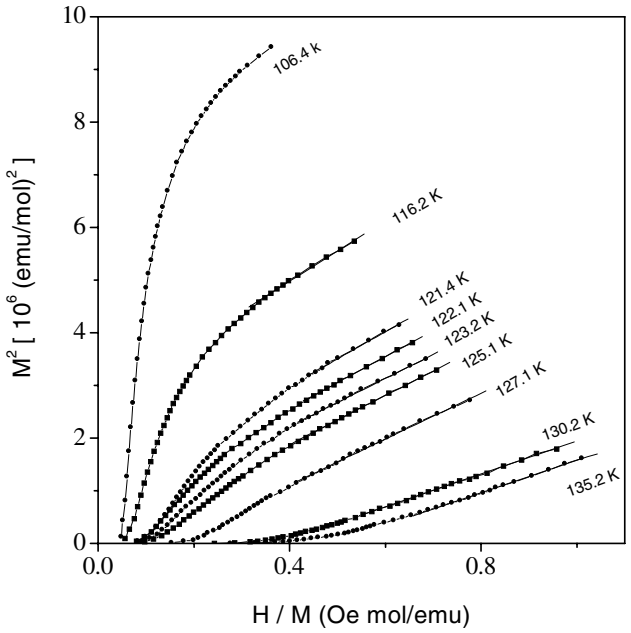

Figure 5. Representative Arrott plots of magnetization isotherms for the sample with $x = 20\%$ in the series $LaMn_{1-x}Al_xO_{3+\delta}$. High field linear fits are indicated by straight lines.

the samples with $x \geqslant 15\%$ where there is no DE to explain the ferromagnetic T_C. Such a situation arises when the nuclear vibrational energies are much lesser than the JT stabilization energy which leads to the resonance between two equivalent nuclear configurations. The relevant vibrational mode is that of the anion oxygen layer between two Mn layers. In fact Millis *et al* had predicted that these dynamic JT distortions are associated with large rms oxygen displacements around the magnetic transition [10] and this prediction was confirmed in neutron diffraction and EXAFS studies [11, 13]. Since Al^{3+} is nonmagnetic, its bonds with Mn^{3+} and Mn^{4+} ions are neglected in the evaluation of magnetic properties. Next, to estimate the strength of these three interactions, we note that the observed T_C is a value resulting from a balance between all these interactions. However, the fraction of these different bonds depends both on the net amount and the distribution of the magnetic ions Mn^{3+} and Mn^{4+}. If the fraction Mn^{4+} is denoted by 'y' then the fraction of Mn^{3+} in the lattice is given by $(1 - x - y)$, where x is the doped Al^{3+} content. Then there would be $(1 - x - y)^2$ Mn^{3+}–Mn^{3+} neighbours, (y^2) Mn^{4+}–Mn^{4+} neighbours and finally $2y(1 - x - y)$ Mn^{3+}–Mn^{4+} neighbours. Thus we can express the mean field T_C in the following form:

$$T_C = (1 - x - y)^2 J_1 - y^2 J_2 + 2y(1 - x - y) J_3 \tag{1}$$

where the exchange constants are expressed in kelvin. By taking the observed T_C values for all the samples with the corresponding x and y values from table 1, we obtain a set of equations which can be simultaneously solved to give the exchange constants. By solving the three equations for $x = 0$, 2.5 and 20% samples, we arrive at the following values: $J_1 = +197.9$ K; $J_2 = -246.0$ K; $J_3 = +368.5$ K. These values are qualitatively similar to those of Jonker's work in the case of LaSrMnO and LaCaMnO systems [1]. The essence is that the DE FM bond is the strongest of the three and the other two bonds are comparable in strength. In the whole analysis it has been assumed that the exchange constants J_1, J_2 and J_3 are constants over the

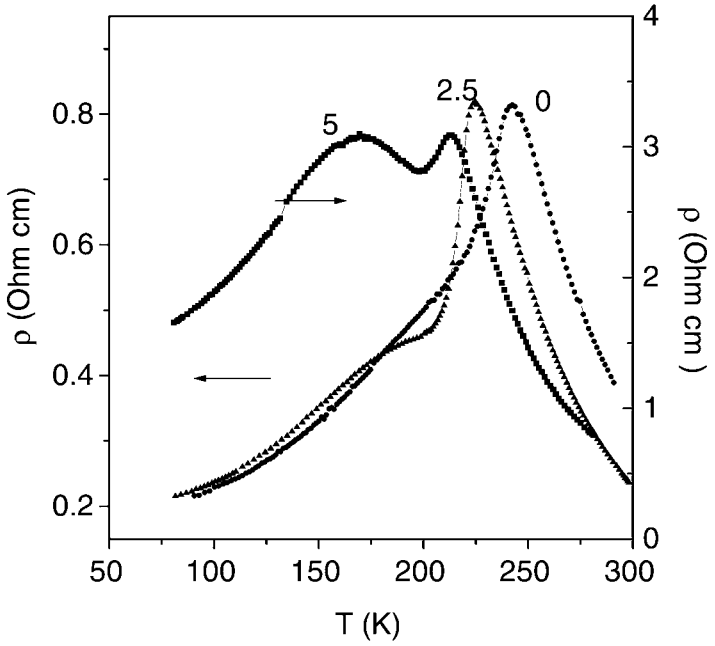

(a)

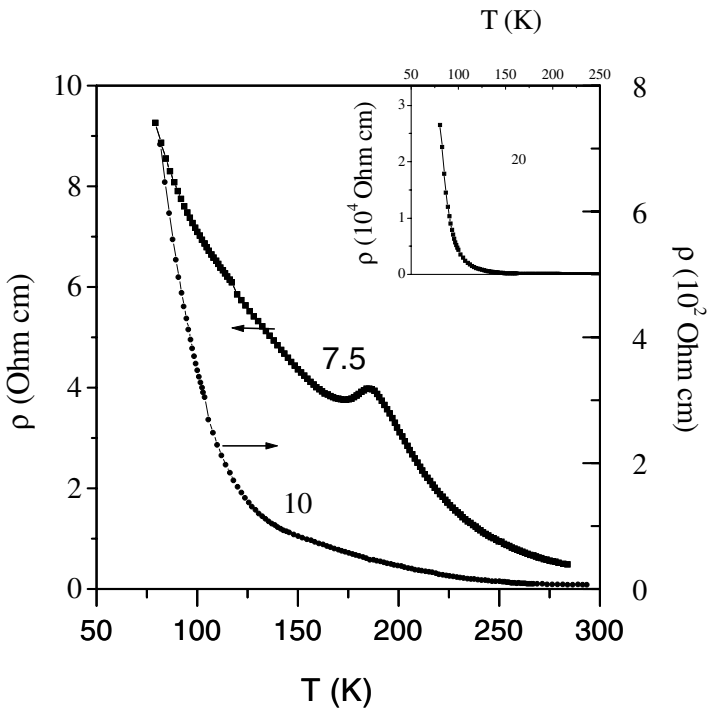

(b)

Figure 6. (a) Temperature dependence of dc resistivity of the $x = 0$, 2.5 and 5% samples of the series $LaMn_{1-x}Al_xO_{3+\delta}$. (b) Temperature dependence of dc resistivity of the $x = 7.5$ and 10% samples of the series $LaMn_{1-x}Al_xO_{3+\delta}$. The inset shows the temperature dependence of dc resistivity of $x = 20\%$ sample.

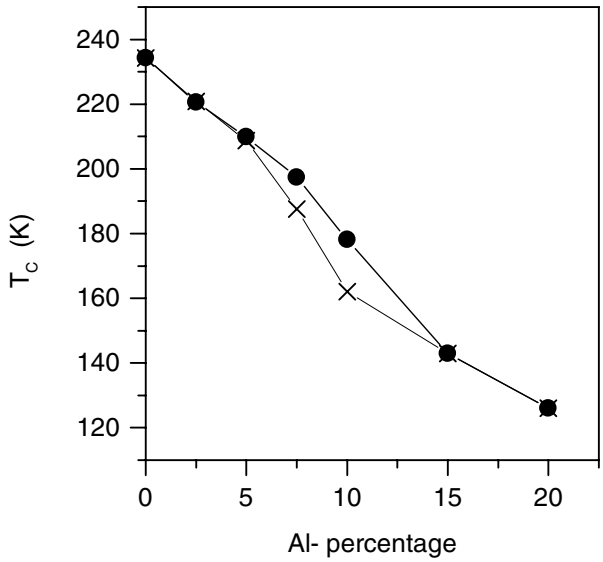

Figure 7. The dependence of T_C on Al doping. The (×) symbols correspond to the experimental data and (●) correspond to calculated values according to equation (1) in the text.

whole composition range which is reasonably valid in the first approximation. However in the finer analysis it may become necessary to relax these exchange constants to be variable due to Al doping in the Mn sublattice. To verify the validity of these estimates we have calculated the T_C for the whole series of samples and we find a reasonably good agreement with the experimental T_C as can be seen in figure 7.

Now it is straightforward to explain our experimental results as an interplay of these three interactions. For $0 \leqslant x \leqslant 5\%$ it is certain that J_3 is dominant in determining the FM due to strong DE interactions. In this region the Mn^{4+} content is much beyond the threshold for DE to take over and the DE strength is nearly the same for all the three samples. The dominance of DE is also indicated by the metallic ferromagnetic state in these samples. The decrease in T_C in this regime can be understood as due to the dilution of the Mn sublattice by Al substitution in the DE framework. It seems that in this composition range, the Al^{3+} substitution replaces both Mn^{3+} and Mn^{4+} ions in equal probability which can be seen from the ratios of (Mn^{3+}/Al^{3+}) and (Mn^{4+}/Al^{3+}). These ratios have a similar functional dependence with x for $x \leqslant 5\%$ (not shown) but have a marked difference beyond $x \geqslant 7.5\%$. In the latter case, the rate at which Mn^{4+} is depleted by Al^{3+} substitution is substantially larger than that at which Mn^{3+} is depleted by Al^{3+} ions. It is worth recalling from table 1 that only in this region of Al substitution, the samples have a clear tendency to become more stoichiometric retaining the rhombohedral structure. This is in contrast to the undoped stoichiometric compound which stabilizes the orthorhombic structure. This has a profound influence on the magnetic interactions in the compounds. DE strength is primarily decided by the (Mn^{3+}/Mn^{4+}) ratio. It is therefore clear that the faster decrease of T_c for $x \geqslant 7.5\%$ is due to the faster rate at which DE bonds are severed and thus J_3 becomes less and less effective with Al substitution in this composition range. As DE has diminished to a greater extent for $x = 7.5$ and 10%, the only effective interaction is the ferromagnetic SE interaction in Mn^{3+}–Mn^{3+} and this is solely responsible for the ferromagnetism of samples with $x \geqslant 15\%$. Thus we demonstrate the importance of ferromagnetic Mn^{3+}–O–Mn^{3+} SE interactions coupled with dynamic JT distortions in higher

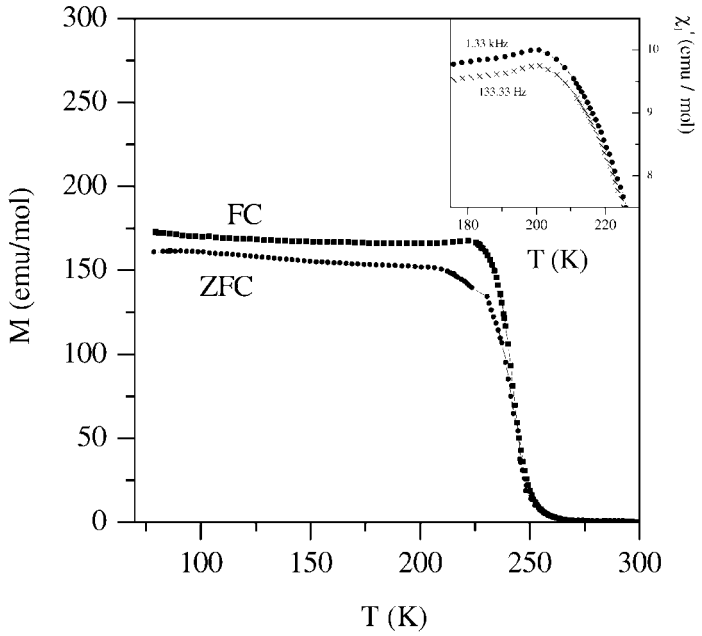

Figure 8. The temperature dependence of zero-field-cooled (ZFC) and field-cooled (FC) magnetization curves of the $x = 0\%$ sample of the series $LaMn_{1-x}Al_xO_{3+\delta}$. The inset shows the frequency dependence of ac susceptibility at 133.33 Hz and 1.33 kHz for the same sample.

doped samples ($x \geqslant 15\%$) where there is no DE at all. More important, even in lower doped samples ($x \leqslant 7.5\%$) where there are predominant DE interactions, one needs to take into account these ferromagnetic SE interactions to reproduce the observed T_C as was done in our semiquantitative analysis. This is precisely the same situation as in prototype CMR manganites and our present findings validate the current wisdom that DE alone is not adequate for explaining FM/metallicity in these systems.

The nature of the second transition at lower temperatures observed for samples with $x \geqslant 7.5\%$ is yet to be ascertained. In the preliminary study, we have observed for the $x = 10\%$ sample that the susceptibility of the second phase is both frequency and field dependent. Further dc magnetization measurements revealed a history dependence of magnetization showing bifurcation in zero-field-cooled (ZFC) and field-cooled (FC) cycles. However, it is not justifiable to attribute this to a signature of frustrated (spin glass like) systems as was done earlier [16]. It is necessary to undertake detailed measurements to ascertain the origin of this second phase uniquely in all the higher doped samples similar to what was done in [22]. For instance, we observe frequency, field and history dependences even in the undoped compound ($x = 0\%$) (figure 8) which exhibits a reasonably clean ferromagnetic transition. Thus effects of granularity and domain wall dynamics have to be kept in mind while interpreting the results. At present we hypothesize that this second transition can be attributed to the dynamics of smaller ferromagnetic clusters arising out of the dilution of ferromagnetic bonds in the infinite ferromagnetic matrix by means of random Al substitution. These clusters are more likely to have a size distribution and hence a distribution in relaxation times that are comparable with the experimental probe times. This can be manifest as the observed frequency dependence in ac susceptibility. The ZFC/FC bifurcation in dc magnetization may be due to progressive freezing of these clusters in a random direction (ZFC) or in the field direction (FC). There are also other

views in the literature that heterogenous canting of ferromagnetic moments in the system can give rise to the mixed magnetic phases which may have different transition temperatures [23].

In conclusion we have synthesized an entirely new series of rhombohedral compounds, $LaMn_{1-x}Al_xO_{3+\delta}$ where we have observed a continuous transition from ferromagnetic–metallic to ferromagnetic–insulating state with increasing Al substitution thereby indicating a cross-over from the DE dominated regime to SE regime within the same structure and the importance of dynamic Jahn–Teller effects coupled with Mn^{3+}–O–Mn^{3+} interactions is shown in establishing ferromagnetism in the whole series. Since the prototype CMR manganites crystallize in rhombohedral and cubic structures, the present series of compounds forms a unique platform to understand magnetic and electron transport properties of these compounds in general.

Acknowledgments

We are grateful to Dr B A Dasannacharya for his keen interest in the work and many useful discussions. We acknowledge Professor M S Hegde, Dr Vasant Sathe and Dr Ashna Bajpai for their initial help in iodometric titrations, Rietveld profile refinement program and ac susceptibility measurements respectively. RVK acknowledges UGC, India for a fellowship.

References

[1] Jonker G H and Van Santen J H 1950 *Physica* **16** 337
Jonker G H 1950 *Physica* **16** 599
Jonker G H 1956 *Physica* **22** 707
[2] Goodenough J B 1955 *Phys. Rev.* **100** 564
Kanamori J 1959 *J. Phys. Chem.* **10** 87
[3] Wollan E O and Koehler W C 1955 *Phys. Rev.* **100** 545
[4] Goodenough J B and Loeb A L 1955 *Phys. Rev.* **98** 391
[5] Ramirez A P 1997 *J. Phys.: Condens. Matter* **9** 8171 and references therein
Coey J M D, Viret M and von Molnar S 1999 *Adv. Phys.* **48** 167 and references therein
[6] Goodenough J B 1997 *J. Appl. Phys.* **81** 5330
[7] Goodenough J B, Wold A, Arnot R J and Menyuk N 1961 *Phys. Rev.* **124** 373
[8] Sturge M D 1967 *Solid State Physics* vol 20 (New York: Academic) p 91
[9] Zener C 1951 *Phys. Rev.* **82** 403
[10] Millis A J, Littlewood P B and Shraiman B I 1995 *Phys. Rev. Lett.* **74** 5144
[11] Dai P, Zhang Jiandi, Mook H A, Liou S H, Dowben P A and Plummer E W 1996 *Phys. Rev.* B **54** R3694
[12] Argyriou D N, Mitchell J F, Potter C D, Bader S D, Kleb R and Jorgensen J D 1997 *Phys. Rev.* B **55** R11 965
[13] Zhao G, Conder K, Keller H and Muller K A 1996 *Nature* **381** 676
Tyson T A, Mustre de Leon J, Conradson S D, Bishop A R, Neumeier J J, Roder H and Zhang Jun 1996 *Phys. Rev.* B **53** 13 985
[14] Subramanian M A, Toby B H, Ramirez A P, Marshall W J, Sleight A W and Kwei G H 1996 *Science* **273** 81
[15] Ghosh K, Ogale S B, Ramesh R, Greene R L, Venkatesan T, Gapchup K M, Bathe Ravi and Patil S I 1999 *Phys. Rev.* B **59** 533
[16] Blasco J, Garcia J, de Teresa T M, Ibarra M R, Pererz J, Algarabel P A, Marquina C and Ritter C 1997 *Phys. Rev.* B **55** 8905
Damay F, Maignan A, Martin C and Raveau B 1997 *J. Appl. Phys.* **82** 1485
Sun J R, Rao G H, Shen B G and Wong H K 1998 *Appl. Phys. Lett.* **73** 2998
[17] Young R A, Sakthivel A, Moss T S and Paivasantos C O 1994 *User's Guide to Program DBWS-9411* (Atlanta, GA: Georgia Institute of Technology)
[18] Van Roosmalen J A M, Cordfunke E H P, Helmholdt R B and Zandbergen H W 1994 *J. Solid. State Chem.* **110** 100
[19] Krishnan R V and Banerjee A 1999 *Rev. Sci. Instrum.* **70** 85
[20] Bajpai A and Banerjee A 1997 *Rev. Sci. Instrum.* **68** 4075

[21] Arrott A 1957 *Phys. Rev.* **108** 1394
[22] Bajpai A and Banerjee A 1997 *Phys. Rev.* B **55** 12 439
[23] Arovas D P and Guinea F 1998 *Phys. Rev.* B **58** 9150